Appl Biochem Biotechnol (2014) 174:926–935
DOI 10.1007/s12010-014-1179-5

Chitosan-Modified Carbon Nanotubes-Based Platform for Low-Density Lipoprotein Detection

Md. Azahar Ali · Nawab Singh · Saurabh Srivastava · Ved V. Agrawal · Renu John · M. Onoda · Bansi D. Malhotra

Received: 1 February 2014 / Accepted: 15 August 2014 /
Published online: 9 September 2014

Abstract We have fabricated an immunosensor based on carbon nanotubes and chitosan (CNT-CH) composite for detection of low density lipoprotein (LDL) molecules via electrochemical impedance technique. The CNT-CH composite deposited on indium tin oxide (ITO)-coated glass electrode has been used to covalently interact with anti-apolipoprotein B (antibody: AAB) via a co-entrapment method. The biofunctionalization of AAB on carboxylated CNT-CH surface has been confirmed by Fourier transform infrared spectroscopic and electron microscopic studies. The covalent functionalization of antibody on transducer surface reveals higher stability and reproducibility of the fabricated immunosensor. Electrochemical properties of the AAB/CNT-CH/ITO electrode have been investigated using cyclic voltammetric and impedimetric techniques. The impedimetric response of the AAB/CNT-CH/ITO immunoelectrode shows a high sensitivity of 0.953 Ω/(mg/dL)/cm^2 in a detection range of 0–120 mg/dL and low detection limit of 12.5 mg/dL with a regression coefficient of 0.996. The observed low value of association constant (0.34 $M^{-1}s^{-1}$) indicates high affinity of AAB/CNT-CH/ITO immunoelectrode towards LDL molecules. This fabricated immunosensor allows quantitative estimation of LDL concentration with distinguishable variation in the impedance signal.

M. A. Ali · N. Singh · S. Srivastava · V. V. Agrawal (✉) · B. D. Malhotra (✉)
Department of Science and Technology Centre on Biomolecular Electronics, CSIR-National Physical Laboratory, Dr. K. S. Krishnan Marg, New Delhi 110012, India
e-mail: ved.varun@gmail.com
e-mail: bansi.malhotra@gmail.com

M. A. Ali · R. John (✉)
Indian Institute of Technology Hyderabad, Ordnance Factory Estate, Yeddumailaram, Hyderabad, AP 502205, India
e-mail: renujohn@iith.ac.in

M. Onoda
Department of Electrical Engineering and Computer Sciences, University of Hyogo, Himeji, Hyogo 671-2280, Japan

B. D. Malhotra
Department of Biotechnology, Delhi Technological University, Shahbad, Daulatpur, Main Bawana Road, Delhi 110042, India

Keywords Low density lipoprotein · Impedance spectroscopy · Carbon nanotubes · Chitosan · Nanocomposite

Introduction

In recent years, the carbon nanotubes (CNTs) and their composites have been extensively used for biomedical applications such as biosensors, tissue engineering, intracellular analysis, cardiovascular systems, dental implants etc. [1, 2]. CNTs consisting of cylindrical graphite sheets having a diameter in nanometre scale and show many attractive properties, including excellent electrochemical behaviour [3]. CNTs can be utilized as an excellent candidate for construction of the electrochemical biosensors owing to their large surface area, high catalytic and electronic conductivity, high mechanical resistance and tunable surface properties [4]. Additionally, CNTs are being explored for application in fuel cells, solar cells and photovoltaics [5]. Due to the presence of abundant functional groups (−COOH, NH_2 etc.), CNTs provide suitable platform for biofunctionalization [6]. Acid treatment of CNTs' sidewalls plays an important role to introduce these functional groups which help towards antibody functionalization via covalent interaction [7]. The biomolecules such as antibodies, enzymes, DNA, PNA and aptamer-functionalized CNTs surface can improve the electronic properties of CNTs for fabrication of electrochemical biosensors [8]. The covalent binding of CNTs with biomolecules via diimide-activated amidation may improve stability and reproducibility of a biosensor. Thus, CNTs can be utilized for amplification of electronic signals for a desired biosensor [1–8].

The poor solubility and agglomeration of CNTs in an aqueous media is currently a major concern [9]. In this context, the biopolymers such as chitosan (CH) play an important role to reduce dispersion or agglomeration of CNTs thereby improving characteristics of the biosensor devices [10–12]. CH displays excellent film-forming ability due to good adhesion, and can be easily decorated with CNTs due to available reactive hydroxyl and amino functional groups [13, 14]. Spinks et al. have observed improved CNTs dispersion by introducing chitosan solution via sonic agitation and then centrifuge to remove CNTs aggregation [13]. The controlled decoration of CNTs with CH can create new CNT-CH nanocomposite hybrid material to develop biosensors [11]. Cao et al. have described the covalent interaction between CH and CNTs for the formation of nanocomposite material [15]. Only a few researchers have reported this CNT-CH nanocomposite for biosensor applications. Luo et al. have developed a biosensor based on CH-entrapped CNTs via electrochemical deposition method [16]. It has been found that this CNT-CH exhibits excellent electrocatalytic properties during reduction and oxidation of hydrogen peroxide. Qiu et al. have reported a glucose biosensor using porous CNT-CH film-modified electrode [17]. The controllable electrodeposition of carbon nanofiber-doped CH biocompatible layer has been used as an electrode material for the cytosensing of K562 cells [18]. A composite of CNT-CH was used as a matrix for the entrapment of lactate dehydrogenase onto a glassy carbon electrode to fabricate lactate biosensor [14]. This reported biosensor provides a fast response, excellent sensitivity, low electro-oxidation potential of NADH, and the alleviation of electrode surface fouling. Thus, chitosan can be entrapped with CNTs to reduce its agglomeration and suitable for electrode material to improve the characteristics of the biosensing device.

In this paper, we have fabricated the carboxylated CNT-CH nanocomposite-based electrode for antibody (anti-apolipoprotein B (AAB)) functionalization via a co-entrapment method. The structural and biofunctionalization have been confirmed using various spectroscopic and microscopic techniques. The antibody functionalized CNT-CH immunoelectrode has been used to detect low density lipoprotein (LDL) molecules via impedance spectroscopic

technique. The immune reaction between AAB and LDL molecules on transducer surface forms immuno-complex which changes the impedance signal during detection. In the blood stream, LDL molecules can carry 60–70 % of the total serum cholesterol. Higher levels of LDL are known to cause heart attack, stroke, hypercholesterolemia and cardiovascular disease. Thus, the estimation of LDL cholesterol is considered very important for clinical diagnostics.

Experimental Section

Reagents All chemicals including chitosan, N-hydroxisuccimide (NHS), N-ethyl-N′-(3-dymethylaminopropyl carbodiimide), anti-apolipoprotein B 100 and low-density lipoprotein (LDL) molecules are of analytical grade and have been purchased from Sigma Aldrich, USA. Five milligrammes of lyophilized LDL powder is dissolved in 2 mL of de-ionized water which containing 150 mM NaCl of pH 7.4 and 0.01 % EDTA. Bovine serum albumin (BSA, 2 mg/mL) solution is prepared in 50 mM phosphate buffer saline (PBS) of pH 7.4 containing 150 mM NaCl. AAB solution (1 mg/mL) is prepared in PBS solution (50 mM) of pH 7.4 containing 150 mM NaCl. Indium tin oxide (ITO)-coated glass slides (film thickness=~150–300 Å; a resistance of 70–100Ω/square) are procured from Vin Karola Instrument.

Fabrication of CNT-CH Immunoelectrode

The CNTs (90 %) are synthesized by catalytic chemical vapour deposition according to a previous report [19]. Five milligrammes of prepared CNTs is dispersed in 4 mL acetate buffer solution (0.05 M, pH 4.2) and sonicated for 6 h resulting in colloidal CNTs solution. A CH (0.50 %) solution is prepared by dissolving CH (50 mg) in 100 mL of acetate buffer solution. Then, 0.5 mL of CNTs colloidal solution is added to 1 mL chitosan solution and sonicated for 2 h resulting in CNT-CH nanocomposite solution. Fifty microlitres of the prepared CNT-CH nanocomposite solution is uniformly spread on ITO surface via drop casting method and is kept at 30 °C for 6 h. The $-NH_2$ groups present in chitosan are utilized to make the covalent bond formation with −COOH groups of CNTs. In addition, due to opposite charge on CH (positive) and CNTs (negative), the electrostatic interaction may also possible to form nanocomposite. This electrode has been used for biofunctionalization.

Antibody Functionalization

A co-entrapment method (two-step method) along with physical adsorption has been utilized for antibody functionalization followed by 1-ethyl-3-(3-dimethylaminopropyl)carbodiimide (EDC)-NHS coupling chemistry. The prepared AAB solution (1 mg/mL) is entrapped on CNT-CH surface for overnight in a humid chamber (at 4 °C) followed by washing with PBS containing 0.05 % in order to remove any unbound AAB. The AAB/CNT-CH/ITO surface is treated with EDC-NHS in which EDC (0.2 M) works as a coupling agent and NHS (0.05 M) works as an activator. EDC-NHS activates the −COOH group in CNTs. This results in formation of C–N bond between the −COOH group of CNT and the $-NH_2$ terminal of AAB. Lastly, 2 mg/dL of BSA solution is used for blocking the nonspecific adsorption of antibodies on AAB/CNT-CH/ITO surface. The prepared bioelectrode is stored at 4 °C when not in use. It has been found that the AAB/CNT-CH/ITO bioelectrode shows high catalytic

behaviour in phosphate buffer saline at pH 7.4 (50 mM, 0.9 % NaCl) containing $[Fe(CN)_6]^{3-/4-}$ (5 mM).

Instrumentation

The surface morphological studies have been investigated using scanning electron microscope (SEM, LEO-440). Fourier transform infrared spectroscopic (FT-IR; PerkinElmer, Model 2000) measurements is confirmed the antibody functionalization on the CNT-CH surface. The electrochemical investigations such as cyclic voltammetry and electrochemical impedance spectroscopy (EIS) have been carried out using an Autolab Potentiostat/Galvanostat (Eco Chemie, The Netherlands) in phosphate buffer saline [PBS, (50 mM, pH 7.0, 0.9 % NaCl)] containing $[Fe(CN)_6]^{3-/4-}$ (5 mM).

Results and Discussions

Morphological Studies

The high-resolution transmission electron microscopy (HR-TEM) image shows an individual CNT and the diameter of CNTs varies from 40 to 100 nm [Fig. 1(i)]. The length of this CNT is in micron range and the central core diameter of this CNT is very small (~16 nm). Inset shows CNTs with different diameters. The atomic scale image shows that CNTs are highly crystalline in nature, with an interlayer spacing of 0.34 nm (d_{002} for CNT, shown in the inset). Thus, it can be concluded that the prepared COOH-functionalized CNTs are multiwalled. The scanning electron micrograph (SEM) studies are carried out at an accelerating voltage of 20 kV [Fig. 1(ii)]. The length range of the COOH-functionalized CNTs is several micrometres, and they have an external diameter of approximately 30–110 nm. These COOH-functionalized CNTs that are likely randomly oriented on the ITO substrate.

FT-IR Studies

The FT-IR spectra of CH (spectra a) shows the bands in the region 3,200–3,500/cm due to the stretching vibration mode of OH groups [Fig. 2(i)]. The IR band at 1,602/cm corresponds to

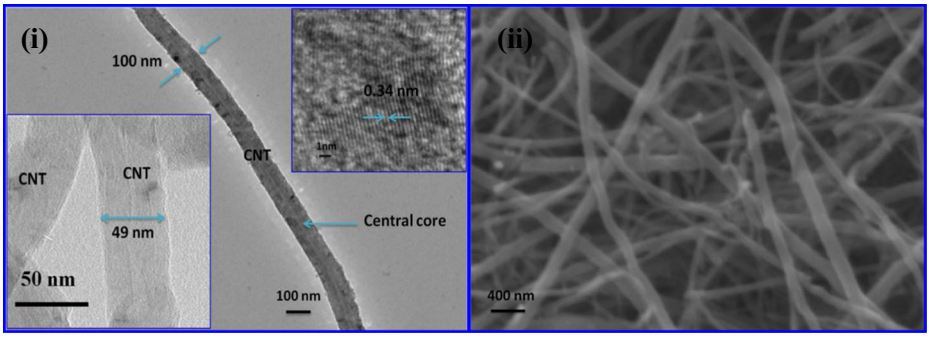

Fig. 1 The HR-TEM analysis of (*i*) an individual CNT (*inset* the CNT with different diameter and lattice fringes of the CNT). (*ii*) SEM image of CNTs

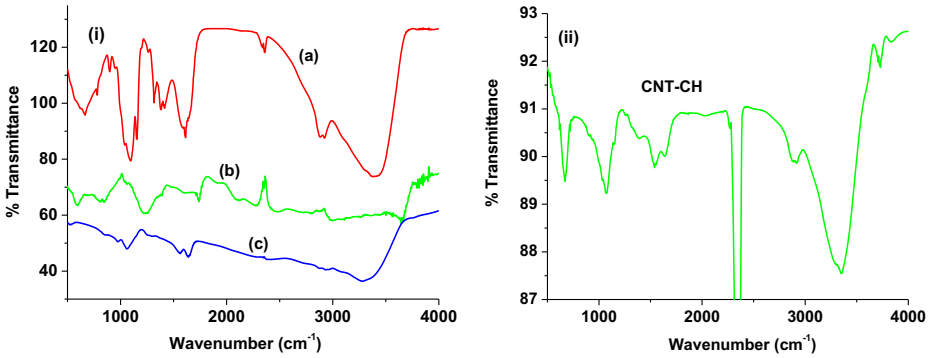

Fig. 2 (*i*) FT-IR spectra of (*a*) CH/ITO film, (*b*) CNT/ITO film and (*c*) AAB/CNT-CH/ITO film. (*ii*) FT-IR spectra of CNT-CH/ITO film

amide I group. The 1,400/cm peak is due to C–N axial deformation (amine group band), 1,317/cm peak is due to COO− group and 1,084/cm is attributed to the stretching vibration mode of the hydroxyl group. In the carboxyl functionalized CNT/ITO film (curve b), the band seen at 840 cm/^{1} is assigned to C–H bending vibration, while those seen at 1,233 and 1,600/cm correspond to stretching vibration of C–C and C=C, bond, respectively. The sharp and strong band found at 1,735/cm is attributed to C=O stretching vibration while a weak band that is seen at 1,233/^{1} due to C–O stretching indicating the carboxyl functionalization of CNTs. Curve (ii) shows the IR spectrum for CNT-CH film. Most peaks appearing in the spectra are combinations of CNT and CH indicating the formation of nanocomposite. However, after immobilization of BSA-AAB on CNT-CH/ITO film surface (curve c), the amide (I and II) bands observed at 1,557 and 3,270/cm, respectively, reveal biofunctionalization.

Electrochemical Studies

Cyclic voltammetry (CV) studies have been conducted for different electrodes in PBS (50 mM, pH 7.0, 0.9 % NaCl) solution containing $[Fe(CN)_6]^{3-/4-}$ in the potential range, −0.7 to +0.7 V verses Ag/AgCl electrode [Fig. 3(i)]. All curves show the well-defined oxidation and reduction peaks in the presence of $[Fe(CN)_6]^{3-/4-}$. The ratio of the cathodic and anodic current is close to 1, which undergoes a quasi-reversible redox process. It has been observed that the peak current for CH/ITO electrode (0.72 mA) is higher compared to that bare CNT/ITO electrode (curve a, 0.57 mA). However, the peak-to-peak potential separation (ΔE) for CH/ITO electrode (curve b, 0.54 V) is found to be lower compared to CNT/ITO electrode (0.82 V) indicating fast electron transfer towards ITO electrode. The drop casted CNTs onto the ITO electrode perhaps lead to slower electron transfer kinetics and poor dispersion ability of CNTs on electrode surface resulting in a large potential for oxidation/reduction of ferro/ferri cyanide molecules. The peak current is enhanced to 0.87 mA for the CNT-CH/ITO electrode due to nanocomposite formation (curve c). Additionally, this may be due to improved electrocatalytic properties of CNTs in presence of CH molecules on the transducer surface. The current decreases due to insulating nature of AAB and BSA loading on CNT-CH/ITO electrode surface (curve d), which perhaps obstruct (or impede) acceleration of the electrons towards the electrode. Figure 3(ii) illustrates the CV of AAB/CNT-CH/ITO immunoelectrode with scan rates varying from 20 to 160 mV/s. There is an increase in both cathodic and anodic peak currents and a slight shift in voltage have been observed with an increase in scan rate. Inset of Fig. 3(ii) shows the variation of anodic peak currents with the scan rate from 20 to

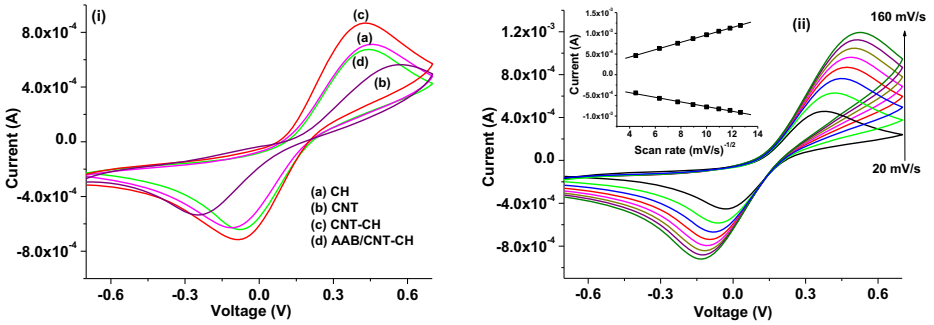

Fig. 3 (*i*) Cyclic voltammetry of different electrodes at scan rate [50 mV/s] and (*ii*) scan rate studies of the AAB/CNT-CH/ITO immunoelectrode

200 mV/s indicating a surface-controlled diffusion process. The surface concentration and diffusivity of the AAB/CysCdS/Au immunoelectrode in presence of redox species has been estimated to be 1.5 μM and 1.34×10^{-7} cm^2/s using Randles-Sevcik Eq. (1).

$$i_p = (269,000)n^{3/2}AD^{1/2}C\nu^{1/2} \tag{1}$$

where i_p is the redox peak current (A), n is the number of electrons transferred in the redox event (1), A is the electrode area (cm^2), D is the diffusion coefficient (cm^2/s), C is the surface concentration (mol) and ν is the scan rate (mV/s). The anodic and cathode current of the scan rate studies are varied according to the Eqs. (2) and (3). The values of the slope, correlation coefficient and intercept of the AAB/CNT-CH/ITO bioelectrode as follows

$$I_{pa} = 0.6\mu A + 0.89\,\mu\text{A} \times \text{sqrt(scan rate)};\ \ R^2 = 0.999 \tag{2}$$

$$I_{ca} = -0.0209\ \ \mu A - 0.56\,\mu\text{A} \times \text{sqrt}\ \ (\text{scan rate});\ \ R^2 = 0.997 \tag{3}$$

Impedance Studies

Electrochemical impedance spectroscopy (EIS) is an efficient technique to describe the electrochemical response of a cell as a function of frequency on application of a small sinusoidal AC signal of frequencies in the ranges of 0.01–10^4 Hz. Various electrodes and impedance responses have been carried out at bias potential 0.01 V to observe the dynamics of antibody–antigen interactions. In a typical Nyquist plot, the impedance (complex value) can be described either by the modulus $|Z|$ and the phase shift φ or by the real part (Z') and the imaginary part (Z'') of the signal. Randles circuit is an equivalent circuit for modelling the EIS experimental data to represent the impedance value. It consists of an electrolyte resistance (R_s), in series with the capacitance of the dielectric layer (C_{dl}), the charge–transfer resistance (R_{ct}) and the Warburg impedance (Z_w). The linear part in this plot, observed in the low-frequency range, indicates a mass transfer-limited process, whereas the semicircle portion, observed in high frequency range, indicates a charge transfer-limited process. The parameter, R_{ct} can be extracted from the fitted circuit model. Figure 4 shows the R_{ct} value of the CH/ITO (a) to be 291 Ω whereas the R_{ct} value of the CNT-CH/ITO (b) is found to be 157 Ω. However, the charge transfer resistance for CNT/ITO electrode is calculated as 997 Ω. Thus, impedance for the CNT-CH/ITO electrode is found to be low compared to other electrodes. This is due to the

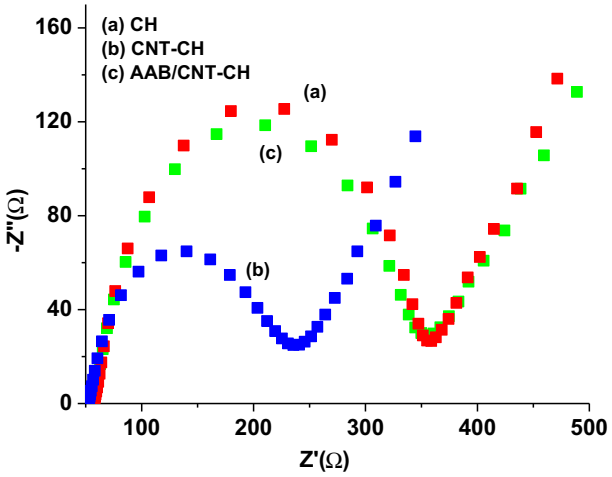

Fig. 4 The Nyquist plots of electrochemical impedance studies for different electrodes

inherent electro-catalytic and enhanced charge transfer properties of CNTs in presence CH molecules. However, the charge transfer properties after biomolecules (AAB-BSA) incorporation on CNT-CH transducer surface is found to be decreased resulting in the enhanced impedance signal (R_{ct} value=285 Ω). This is attributed to the AAB–CNT interaction which impedes the ions transfer from bulk solution to electrode through the diffusion layer and the presence of bulky protein molecules and the steric hindrance of the electron transfer. The heterogeneous electron transfer (k) of the various electrodes has been estimated using charge transfer kinetics as given in Eq. 4

$$k = \frac{RT}{n^2 F^2 A R_{ct} C} \tag{4}$$

where R is the gas constant (8.3145 J/mol), T is the temperature (298 K), n is the electron transferring constant of the redox couple (1), F is the Faraday constant (96485.3 sA/mol), A is the electrode area (0.25 cm^2) and C is the concentration of the redox couple (5 mM). The k_0 values of the AAB/CNT-CH/ITO, CNT-CH/ITO, CH/ITO and CNT/ITO electrodes are obtained as 3.31, 1.8, 3.3 and 12.6×10^{-12} cm/s, respectively.

Impedimetric Response Studies

The impedimetric response for the AAB/CNT-CH/ITO immunoelectrode has been carried out as a function of lipid (LDL) concentration [0–120 mg/dL] in PBS containing $[Fe(CN)_6]^{3-/4-}$ with incubation time of about 4 min [Fig. 5(i)]. The charge transfer resistance (R_{ct}) and double-layer capacitance (C_{dl}) are the most important electrical parameters for analysis of the antibody–antigen interactions. The availability of binding site of antibody (AAB) known as paratope has an affinity to selectively interact with specific binding sites called epitopes of antigen (LDL) resulting in immuno-complex formation. The change in LDL concentration during detection of LDL indicates a change in impedance signal. It is observed that the R_{ct} value increases linearly as LDL concentration increases (0–120 mg/dL) [Fig. 5(ii)]. The increased R_{ct} value indicates that the presence of the insulating layer of LDL on AAB/CNT-CH/ITO immunoelectrode surface due to penetration of the redox species towards the

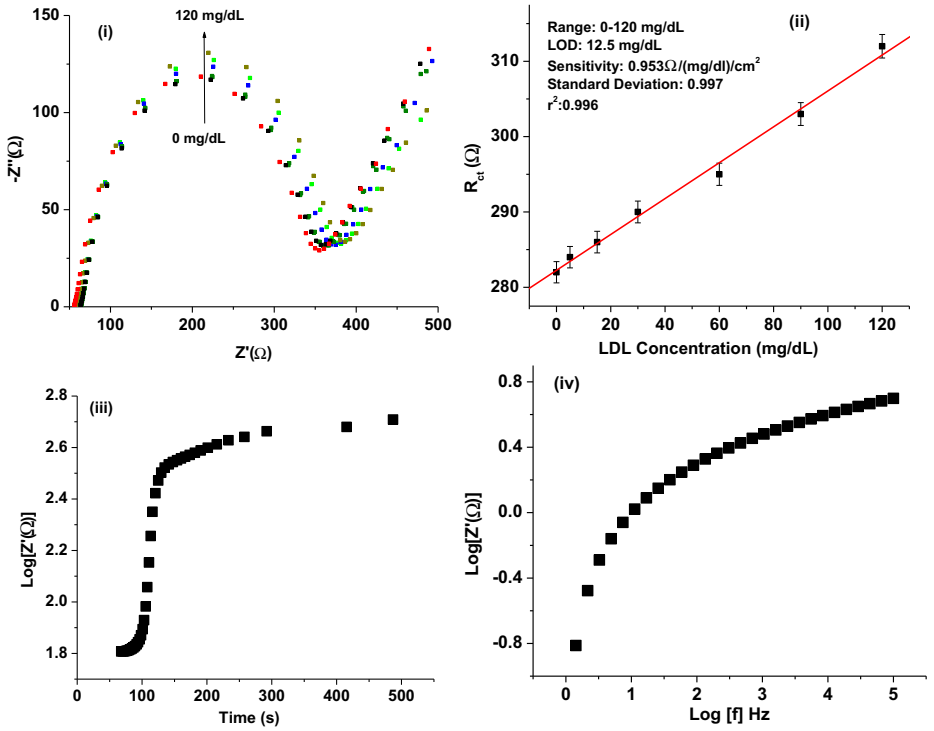

Fig. 5 (*i*) The EIS response of the AAB/CNT-CH/ITO immunoelectrode as a function of LDL concentration (0–120 mg/dL). (*ii*) Sensor calibration plot between the LDL concentration and R_{ct} value. (*iii*) Response time verses impedance plot for 60 mg/dL LDL concentration and (*iv*) Frequencies verses impedance plot for 60 mg/dL of LDL concentration

electrode, resulting in higher diameter of EIS curves. Additionally, the negative charges carried by the LDL phospholipids coating may block the electron transfer of the $[Fe(CN)_6]^{3-/4-}$ redox couple resulting in higher impedance. The immunoelectrode when treated with the 0.2 M glycine solution of pH 2.4 for about 2 min results in 95 % of the regenerated immunoelectrode. The value of R_{ct} of the AAB/CNT-CH/ITO immunoelectrode is varied with LDL concentration (0–120 mg/dL) according to Eq. (5)

$$R_{CT}(\Omega) = 282.2(\Omega) + 0.238\,\Omega/(\mathrm{mg/dL}) \times \text{LDL concentration} \tag{5}$$

The sensitivity of the AAB/CNT-CH/ITO immunosensor is found as $0.953\,\Omega/(\mathrm{mg/dL})/\mathrm{cm}^2$ with regression coefficient (r^2) as 0.996. It can be seen that the impedimetric biosensor exhibits improved characteristics such as low detection limit of 12.5 mg/dL using $3\sigma_b/m$ criteria, where m is the slope of the calibration graph and σ_b is the standard deviation and response time of 130 s [Fig. 5(iii)]. This nanocomposite (CNT-CH)-based electrode for EIS measurement technique is an efficient, simple, low-cost and time-consuming technique for LDL estimation compared to other techniques such as Friedewald calculation, ultracentrification, electrophoresis etc. In addition, the prepared AAB/CNT-CH/ITO immunoelectrode has been used to investigate selectivity test for LDL (60 mg/dL) in the presence of cholesterol oleate (150 mg/dL), triglyceride (150 mg/dL), free cholesterol (150 mg/dL), and all mixed. The results indicate

that there is negligible change (reduced 98.99 %) in the impedance signal with these analytes indicating non-interference. The storage stability of the AAB/CNT-CH/ITO immunoelectrode has been determined by observing the R_{ct} value at regular intervals of time for 50 days. A plot between frequencies and impedance for 60 mg/dL of LDL concentration is shown in Fig. 5(iv). The AAB/CNT-CH/ITO immunoelectrode is stored at 40 °C when not in use. It has been observed that the immunoelectrode exhibits 97 % response up to 43 days.

Conclusions

A biosensor based on anti-apolipoprotein B functionalized CNT-CH nanocomposite has been fabricated to detect LDL molecules using EIS technique. The electrochemical, structural and morphological properties of the prepared CNT-CH nanocomposite have been investigated using EIS, CV, XRD, FT-IR and TEM techniques. The superior electrochemical properties of antibody co-entrapped CNT-CH nanocomposite improve the biosensor efficacy for detection of LDL concentration. The AAB/CNT-CH/ITO immunosensor is found to be selective for LDL and exhibits a wide detection range of LDL (0–120 mg/dL). The CNT-CH nanocomposite provides a biocompatible and favourable environment due to high surface-to-volume ratio resulting in enhanced loading capacity of AAB. Higher stability of the proposed biosensor has been observed due to covalent functionalization of AAB on CNT-CH nanocomposite surface. This AAB/CNT-CH/ITO immunosensor shows higher sensitivity and fast response. The high sensitivity combined with specificity of LDL-AAB binding, towards LDL detection using CNT-CH nanocomposite is an interesting platform that can be used to detect other lipids such as VLDL, triglyceride etc.

Acknowledgments The authors thank Director NPL, New Delhi, India, for the facilities. Md. Azahar Ali is thankful to CSIR, India for the award of Senior Research Fellowship. V. V. A. is thankful to TSDP-DST and CSIR empower project for funding. The financial support received from Department of Science and Technology, India (grant no. DST/TSG/ME/2008/18) and Indian Council of Medical Research, India (grant no. ICMR/5/3/8/91/GM/2010-RHN) is gratefully acknowledged.

References

1. Sinha, N., & Yeow, J. T.-W. (2005). Carbon nanotubes for biomedical applications. *IEEE Transaction Nanbioscience, 4*, 180–195.
2. Yang, W., Thordarson, P., Gooding, J. J., et al. (2007). Carbon nanotubes for biological and biomedical applications. *Nanotechnology, 18*, 412001.
3. Lin, Y., Lu, F., Tu, Y., et al. (2004). Glucose biosensors based on carbon nanotube nanoelectrode ensembles. *Nano Letters, 4*, 191–195.
4. Wang, J., & Lin, Y. (2008). Functionalized carbon nanotubes and nanofibers for biosensing applications. *Trends in Analytical Chemistry, 27*, 619–626.
5. Zhu, H., Wei, J., Wang, K., et al. (2009). Applications of carbon materials in photovoltaic solar cells. *Solar Energy Materials & Solar Cells, 93*, 1461–1470.
6. Balasubramanian, K., & Burghard, M. (2008). Electrochemically functionalized carbon nanotubes for device applications. *Journal of Materials Chemistry, 18*, 3071–3083.
7. Daniel, S., Rao, T. P., Rao, K. S., et al. (2007). A review of DNA functionalized/grafted carbon nanotubes and their characterization. *Sensors and Actuators B, 122*, 672–682.
8. Das, M., Dhand, C., Sumana, G., et al. (2012). Electrophoretically fabricated core-shell CNT-DNA biowires for biosensing. *Journal of Materials Chemistry, 22*, 2727–2732.
9. Vaisman, L., Wagner, H. D., & Marom, G. (2006). The role of surfactants in dispersion of carbon nanotubes. *Advances in Colloid and Interface Science, 128–130*, 37–46.

10. Li, J., Liu, Q., Liu, Y., et al. (2005). DNA biosensor based on chitosan film doped with carbon nanotubes. *Analytical Biochemistry, 346*, 107–114.
11. Liu, Y., Tang, J., Chen, X., et al. (2005). Decoration of carbon nanotubes with chitosan. *Carbon, 43*, 3178–3180.
12. Wu, Z., Feng, W., Feng, Y., et al. (2007). Preparation and characterization of chitosan-grafted multiwalled carbon nanotubes and their electrochemical properties. *Carbon, 45*, 1212–1218.
13. Spinks, G. M., Shin, S. R., Wallace, G. G., et al. (2006). Mechanical properties of chitosan/CNT microfibers obtained with improved dispersion. *Sensors and Actuators B, 115*, 678–684.
14. Tsai, Y.-C., Chen, S.-Y., Liaw, & H.-W., (2007). Immobilization of lactate dehydrogenase within multiwalled carbon nanotube-chitosan nanocomposite for application to lactate biosensors. *Sensors and Actuators B, 125*, 474–481.
15. Cao, X., Dong, H., Ming, C., et al. (2009). The enhanced mechanical properties of a covalently bound chitosan-multiwalled carbon nanotube nanocomposite. *Journal of Applied Polymer Science, 113*, 466–472.
16. Luo, X.-L., Xu, J.-J., Wang, J.-L., et al. (2005). Electrochemically deposited nanocomposite nanotubes for biosensor application. *Chemical Communications, 2169–2171*.
17. Qiu, J.-D., Xie, H.-Y., & Liang, R.-P. (2008). Preparation of porous chitosan/carbon nanotubes film modified electrode for biosensor application. *Microchimica Acta, 162*, 57–64.
18. Hao, C., Ding, L., & Zhang, X. (2007). Biocompatible conductive architecture of carbon nanofiber-doped chitosan prepared with controllable electrodeposition for cytosensing. *Analytical Chemistry, 79*, 4442–4447.
19. Ali, M.A., Srivastava, S., Solanki, P.R. (2013). Highly efficient bienzyme functionalized nanocomposite-based microfluidics biosensor platform for biomedical application. *Scientific Reports, 3*(1–9), 2661.